2020

Parametric Study of a Turbojet Engine With Auxiliary Bypass Combustion- The TurboAux Engine

Kaleab Fetahi
Old Dominion University, kfeta001@odu.edu

Sharanabasaweshwara A. Asundi
Old Dominion University, sasundi@odu.edu

Arthur C. Taylor
Old Dominion University, ataylor@odu.edu

Adem H. Ibrahim

Syed Firasat Ali

Original Publication Citation

Fetahi, K., Asundi, S., Taylor, A., Ali, S. F., & Ibrahim, A. (2020). Parametric study of a turbojet engine with auxiliary bypass combustion – The TurboAux engine. AIAA Propulsion and Energy 2020 Forum, Virtual Event, August 24-28, 2020.

AIAA Propulsion and Energy Forum
August 24-28, 2020, VIRTUAL EVENT
AIAA Propulsion and Energy 2020 Forum

10.2514/6.2020-3709

Parametric Study of a Turbojet Engine with Auxiliary Bypass Combustion – The TurboAux Engine

Kaleab Fetahi[1], Sharanabasaweshwara A. Asundi[2], Arthur C. Taylor[3]
Old Dominion University, Norfolk, Virginia, 23529, United States of America

Syed Firasat Ali[4]
Tuskegee University, Tuskegee, Alabama, 36088, United States of America

Adem H. Ibrahim[5]
Norfolk State University, Norfolk, VA, 23504, United States of America

A parametric study of a novel turbojet engine with an auxiliary combustion chamber, nicknamed the TurboAux engine is presented. The TurboAux engine is conceived as an extension of a turbojet engine with an auxiliary bypass annular combustion chamber around the core stream. The study presented in this article is motivated by the need to facilitate clean secondary burning of fuel at temperatures higher than conventionally realized from air exiting the low-pressure compressor. The parametric study is initiated by performing a simple optimization analysis to identify optimal 'fan' pressure ratios for a series of conventional low-bypass turbofan engines with varying bypass ratios (0.1 to 1.5). The fan pressure ratios for corresponding bypass ratios are chosen for studying varying configurations of the TurboAux engine. The article is presented in two phases – (i) Phase I presents the simulations carried out to arrive at an optimal configuration of a TurboAux engine and it formulation, (ii) Phase II presents simulations and results to compare the performance of a low-bypass turbofan engine to the TurboAux engine. The formulation and results are an attempt to make a case for charter aircrafts and efficient close-air-support aircrafts.

I. Nomenclature

B	=	bypass ratio
C	=	local speed of sound
C_{p0}	=	specific heat at constant pressure
f_{actual}	=	actual fuel to air ratio of core stream
f_{aux}	=	actual fuel to air ratio of auxiliary stream
f_{ideal}	=	ideal fuel to air ratio
f_o	=	overall actual fuel to air ratio of core and auxiliary streams
H_{rpCO2}	=	enthalpy of reaction of CO_2
H_{rpf}	=	enthalpy of reaction of fuel
HV	=	heating value of fuel

[1] Graduate Student, Mechanical and Aerospace Engineering, and AIAA Student Member.
[2] Assistant Professor, Mechanical and Aerospace Engineering, and AIAA Professional Member.
[3] Professor, Mechanical and Aerospace Engineering.
[4] Associate Professor, Aerospace Science Engineering, and AIAA Associate Member.
[5] Professor, Mechanical Engineering, and AIAA Associate Member.

M_a = flight speed
M_{air} = molar mass of air
$\dot{m}_{aux}$ = mass flow of auxiliary stream
$\dot{m}_{core}$ = mass flow of core stream
$\dot{m}_{f1}$ = mass flow of fuel into core stream
$\dot{m}_{f2}$ = mass flow of fuel into auxiliary stream
M_{fuel} = molar mass of fuel
P_0 = stagnation pressure
P_a = ambient static pressure
R = specific gas constant
T_0 = stagnation temperature
T_a = ambient static temperature
T_p = static temperature of the products of combustion
T_r = static temperature of the reactants of combustion
V_a = velocity of air at inlet
w_{CHP} = specific work required to drive high-pressure compressor
w_{CLP} = specific work required to drive low-pressure compressor
Y_{cc} = moles of air required for stoichiometric combustion
γ = ratio of specific heat at constant pressure to specific heat at constant volume
η_b = burner efficiency
η_c = compressor efficiency
η_d = diffuser efficiency
η_m = mechanical efficiency
η_n = nozzle efficiency
η_o = overall efficiency
η_p = propulsive efficiency
η_t = turbine efficiency
η_{th} = thermal efficiency
π_c = overall pressure ratio
π_{HP} = high-pressure compressor pressure ratio
π_{LP} = low-pressure compressor pressure ratio

II. Introduction

Conventional turbojet engines have one stream, which passes through the core of the engine without bypassing any of the components. The core stream is compressed through the various stages of the compressor prior to combustion, then after combustion, is expanded through the various stages of the turbine prior to exhausting through a nozzle. The core stream, after the combustion stage, has a considerable increase in its thermal and kinetic energy. In current operational engines, there are strict limitations on the temperature that the turbine blades can withstand. Temperatures in excess of 1950 K can cause the thin blades of a turbine to melt, which may damage the engine [1,2]. These limitations manifest in the potential thrust capability of an engine. To overcome these limitations, a turbojet engine with an auxiliary bypass combustion chamber, nicknamed TurboAux engine, is conceived and presented as a parametric study in this paper. The parametric study is initiated by performing a simple optimization analysis to identify optimal 'fan' pressure ratios for a series of conventional turbofan engines with varying bypass ratios. The fan pressure ratios (FPRs) for corresponding bypass ratios are chosen for studying varying configurations of the TurboAux engine. This research analyzes the viability of an auxiliary bypass combustion system that could mitigate the issues with efficient energy production. The auxiliary combustion chamber would use oxygen-rich air coming from the low-pressure compressor (LPC) to feed the secondary combustion process instead of just bypassing the engine. The article is organized as follows. A schematic layout and the description of the TurboAux engine are presented in Section III. The simulations carried out to arrive at an optimal configuration of a TurboAux engine are presented in Section IV and the formulation is presented in Section V. The simulations, results to compare the performance of varying configurations of the TurboAux engine to a conventional low-bypass turbofan engine are presented in Section V. As part of this section, the results are used to discuss a case for the TurboAux engine to be used in charter aircrafts and other aircraft with similar engines.

III. Configuration of the TurboAux Engine

A schematic layout of the configuration of the TurboAux engine is shown in Fig. 1. Airflow will enter the inlet of the diffuser of the engine, and the stream will be compressed by the LPC and then the high-pressure compressor (HPC). After the LPC stage, the stream will diverge into two streams where one stream will enter the HPC for further compression and will be ignited in the main combustion chamber while the other stream will bypass the HPC and enter the auxiliary bypass combustion chamber. This stream will also bypass the main combustion chamber and the turbine. The core stream, after exiting the main combustion chamber, will outlet into the various stages of the turbine, which will power the compressors. The bypass stream, upon ignition in the auxiliary combustion chamber will reunite and mix with the core stream prior to exhausting through a common nozzle. Since the auxiliary combustion chamber will not exhaust its hot gases into the turbine, it is free of the temperature limitations that the core stream will experience to avoid damaging the thin blades of the turbine. The bypass stream is an oxygen-rich stream, which will allow for "clean" burning at temperatures in excess of 2500 K. The raising of the temperature of the products of this auxiliary combustion chamber is believed to lead to an increase in the efficiency of the engine

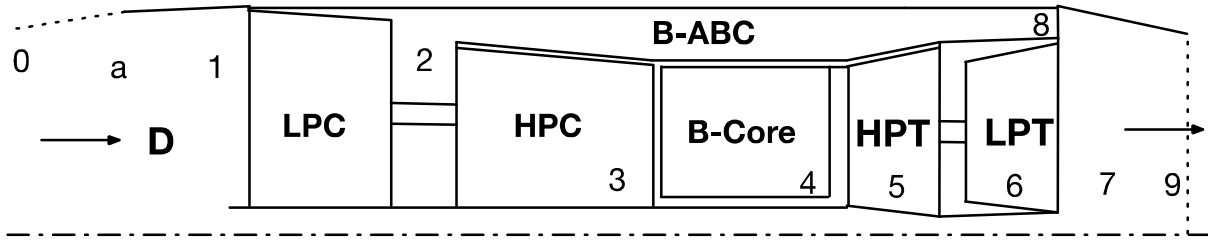

0-1: Free Stream to Engine Entrance
a-1: Diffuser (D)
1-2: Low Pressure Compressor (LPC)
2-3: High Pressure Compressor (HPC)
2-8: Auxiliary Bypass Combustion Burner (B-ABC)
3-4: Core Burner (B-Core)
4-5: High Pressure Turbine (HPT)
5-6: Low Pressure Turbine (LPT)
6&8-7: Mixing
7-9: Single Converging Nozzle (Core+ABC)

Fig. 1 Schematic Layout of the Turbojet Engine with Auxiliary Bypass Combustion: TurboAux Engine

IV. Optimization Analysis to Identify Ideal Fan Pressure (LPC) Ratio

An optimization analysis on a conventional turbofan engine was conducted to identify an optimal FPR and bypass ratio configuration [3], which would be adopted as the auxiliary bypass pressure ratio (ABPR) for the auxiliary bypass combustion chamber of the TurboAux engine. The results of these simulations are summarized in Fig. 2. As part of this optimization analysis, the overall pressure ratio (OPR) and the turbine inlet temperature were maintained constant for a range of bypass ratios of a conventional turbofan engine. For each configuration of the turbofan engine, the fan pressure ratio was varied from 1.3 to 7 and the thrust specific fuel consumption (TSFC) along with the specific thrust (Fs) were computed as shown in Fig. 2. For each bypass ratio, the results of the analysis yielded an optimal fan pressure ratio, where the TSFC was minimized and Fs was maximized, simultaneously. The optimal FPR thus identified was used as the auxiliary bypass pressure ratio of the TurboAux engine.

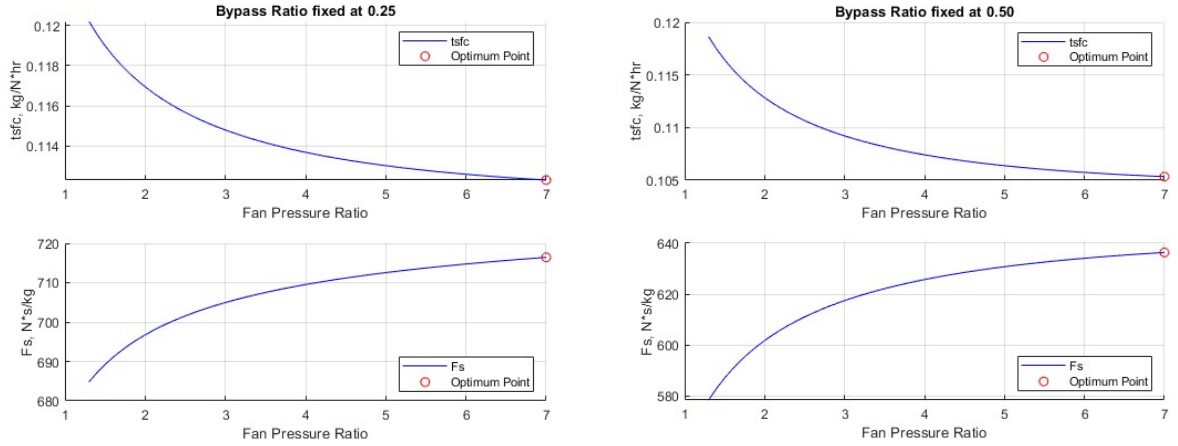

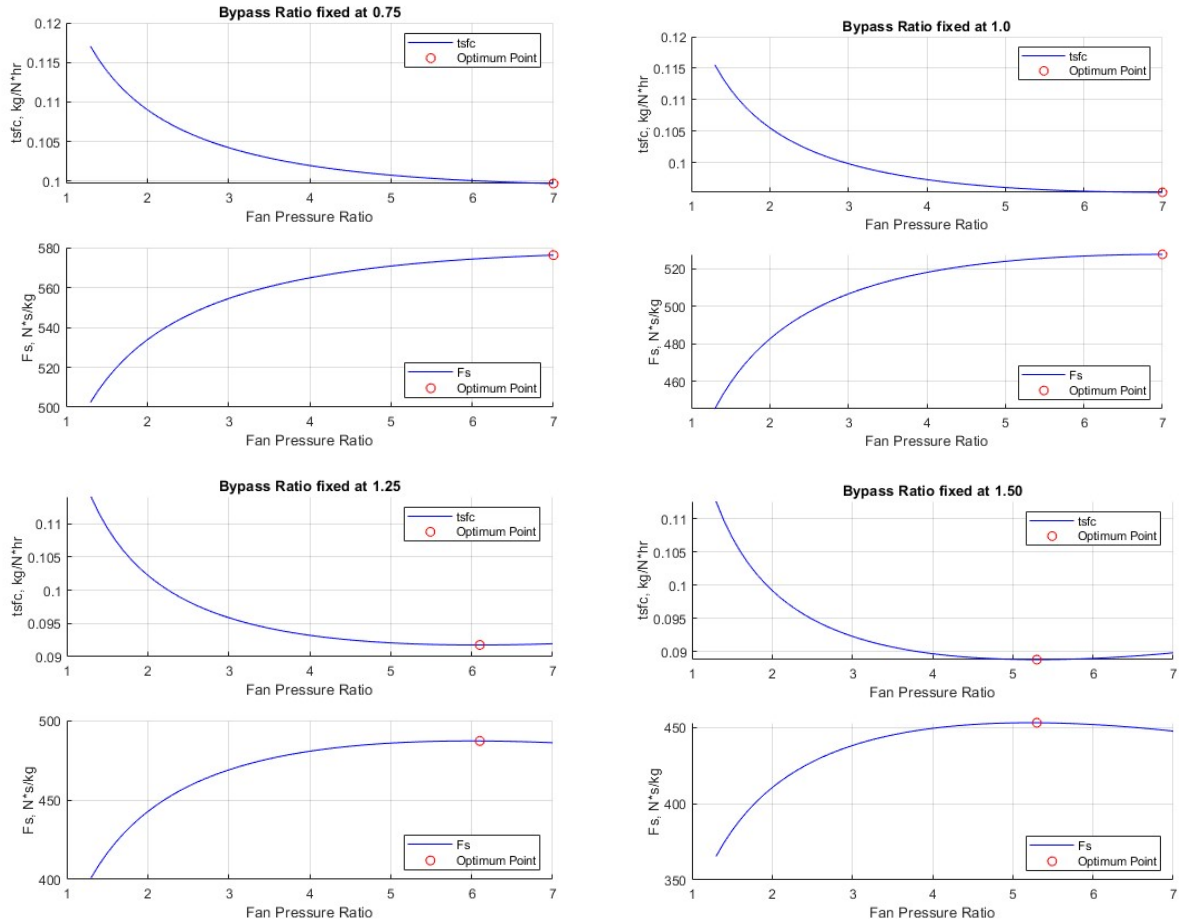

Fig. 2 Optimization Analysis to Identify Optimal Pressure Ratio Corresponding to a Bypass Ratio

V. Formulation

This section is a presentation of the mathematical formulation and calculations performed in the computer program to arrive at the results presented in the next section. Flight conditions and other simulation parameters and properties were selected to coincide with current flight conditions of similar engines and are summarized in Table 1.

Table 1. Simulation Parameters and Flight Conditions.

Flight conditions:	Ma = 0.84	Pa = 54.05 kPa	T_a = 255.7 K
Air properties:	C_{p0air} = 1004.5 J/kg*K	γ_{air} = 1.4	R_{air} = 287 J/kg*K
Gas properties:	C_{p0gas} = 1148 J/kg*K	γ_{gas} = 1.3333	R_{gas} = 287 J/kg*K
Other parameters:	T_{04} = 1922 K	T_{08} = 2516 K	π_c = 50
Efficiencies:	η_d = 0.93	η_c = 0.93	η_b = 0.98
	η_m = 0.99	η_t = 0.90	η_n = 0.95
Fuel properties:	H_{rpf} = -8561991.6 kJ/kmol	M_{fuel} = 197.7 kmol/kg	HV = 43308000 J/kg
	Moles of Carbon (MC) = 14.4	Moles of Hydrogen (MH) = 24.9	Moles of Oxygen (MO) = 0
Other properties:	H_{rpCO2} = 282800 kJ/kmol	M_{air} = 28.97 kmol/kg	

The local speed of sound and the flow speed at the inlet of the of the diffuser are computed in Eqs. (1) and (2), respectively. Upon entering the diffuser, the stream is slowed down and the new stagnation temperature and pressure of the stream due to the reduction in velocity and diffuser efficiency are calculated in Eqs. (3) and (4), respectively.

$$\mathrm{C} = \sqrt{\gamma_\mathrm{a} \cdot \mathrm{R_a} \cdot \mathrm{T_a}} \tag{1}$$

$$\mathrm{V_a} = \mathrm{M_a} \cdot \mathrm{C} \tag{2}$$

$$\mathrm{T_{01}} = \mathrm{T_a}\left[1 + \left(\frac{\gamma_\mathrm{a}-1}{2} \cdot \mathrm{M_a^2}\right)\right] \tag{3}$$

$$\mathrm{P_{01}} = \mathrm{P_a}\left[1 + \eta_\mathrm{d} \cdot \left(\frac{\gamma_\mathrm{a}-1}{2}\right) \cdot \mathrm{M_a^2}\right]^{\frac{\gamma_\mathrm{a}}{\gamma_\mathrm{a}-1}} \tag{4}$$

After the diffuser, the flow is compressed by the LPC or "fan". The stagnation pressure is simply found as the product of the pressure ratio across the fan (FPR). The optimum FPR value from the optimized design is used here in Eq. (5). The stagnation temperature is computed in Eq. (6) which accounts for the efficiency of the compressor and the specific work required to operate the LPC is computed in Eq. (7).

$$P_{02} = P_{01} \cdot \pi_{LP} \tag{5}$$

$$T_{02} = T_{01} + \left\{\frac{T_{01}\left[\left(\pi_{LP}^{\frac{\gamma a-1}{\gamma a}}\right)-1\right]}{\eta_c}\right\} \tag{6}$$

$$W_C^{LP} = (B+1) \cdot C_{p0a} \cdot (T_{01} - T_{02}) \tag{7}$$

Following the compression of the stream in the LPC, the stream diverges into two streams: the core stream and the auxiliary stream. The bypass ratio is defined in Eq. (8). The auxiliary stream bypasses the core of the engine and enters the auxiliary combustion chamber, while the core stream is compressed further through the stages of the HPC. The combustion process of the auxiliary combustion chamber will produce products at a temperature of 2516 K. The loss in stagnation pressure in this combustion process is calculated in Eq. (9).

$$B = \frac{\dot{m}_{aux}}{\dot{m}_{core}} \tag{8}$$

$$P_{08} = P_{02} \cdot (\eta_b) \tag{9}$$

The compression ratio of the HPC is calculated in Eq. (10) as the overall pressure ratio divided by the FPR. The stagnation pressure, stagnation temperature, and specific work required to operate the HPC are computed in similar manner as in the LPC in Eqs. (11), (12), and (13) respectively.

$$\pi_{HP} = \frac{\pi_C}{\pi_{LP}} \tag{10}$$

$$P_{03} = P_{02} \cdot \pi_{HP} \tag{11}$$

$$T_{03} = T_{02} + \left\{\frac{T_{02}\left[\left(\pi_{HP}^{\frac{\gamma a-1}{\gamma a}}\right)-1\right]}{\eta_c}\right\} \tag{12}$$

$$W_C^{HP} = C_{p0a} \cdot (T_{01} - T_{02}) \tag{13}$$

The combustion process is assumed as a complete combustion process with excess air in the products and was modeled in both the auxiliary and main combustion chambers using the enthalpy of reactions, enthalpy of combustion, and the first law of thermodynamics. Equations (14) and (15) are equations used calculate the specific enthalpy, on a molar basis, of each constituent in the combustion process. The constants a, b, and c are experimental coefficients taken from literature used in the calculation of the specific enthalpy [5]. Equation (16) calculates the change in the specific enthalpy. Due to temperature limitations of the turbine blades, the products of combustion from the main combustion chamber are exiting at 1922 K. The number of moles for stoichiometric combustion of the fuel is computed in Eq. (17), and with the fuel, temperature of the reactants, and the temperature of the products specified, the number of moles of air required for complete combustion with excess air in the products is calculated in Eq. (18).

$$\bar{h}_{Tr} = a + b \cdot Tr + c \cdot ln(Tr) \tag{14}$$

$$\bar{h}_{Tp} = a + b \cdot Tp + c \cdot ln(Tp) \tag{15}$$

$$\Delta\bar{h} = \bar{h}_{Tp} - \bar{h}_{Tr} \tag{16}$$

$$Y_{cc} = MC + \left(\frac{MH}{4}\right) - \left(\frac{MO}{2}\right) \tag{17}$$

$$y = \frac{-Hrp_f - (MC)\Delta\bar{h}_{CO_2} - \left(\frac{MH}{2}\right)\Delta\bar{h}_{H_2O} + (Y_{cc})\Delta\bar{h}_{CO_2}}{(3.76)\Delta\bar{h}_{N_2} + \Delta\bar{h}_{O_2}} \tag{18}$$

After the number of moles of air required for complete combustion is calculated in Eq. (18), Eq. (19) computes the ideal fuel to air ratio on a mass basis. To account for non-ideal combustion, the actual fuel to air ratios for both the main combustion chamber and the auxiliary combustion chamber are computed in Eqs. (20) and (21) respectfully. Losses in stagnation pressure due to friction and combustion are calculated in Eq. (22). Conservation of mass states that the total mass flow rate of fuel is the sum of the separate mass flow rates in Eq. (23). Using the bypass ratio, the overall fuel to air ratio of the entire engine accounting for both combustion processes is calculated in Eq. (24).

$$f_{ideal} = \left(\frac{1}{4.76 \cdot y}\right)\left(\frac{M_{fuel}}{M_{air}}\right) \tag{19}$$

$$f_{actual} = \frac{f_{ideal}}{\eta_b} = \frac{\dot{m}_{f1}}{\dot{m}_{core}} \tag{20}$$

$$f_{aux} = \frac{f_{ideal}}{\eta_b} = \frac{\dot{m}_{f2}}{\dot{m}_{aux}} \tag{21}$$

$$P_{04} = P_{03} \cdot (\eta_b) \tag{22}$$

$$\dot{m}_{ftot} = \dot{m}_{f1} + \dot{m}_{f2} \tag{23}$$

$$f_o = \left(\frac{B \cdot f_{aux}}{B+1}\right)\left(\frac{f_{actual}}{B+1}\right) = \frac{\dot{m}_{ftot}}{\dot{m}_{core}} \tag{24}$$

Upon exiting the main combustion chamber, the core stream will be expanded through the high-pressure turbine and the low-pressure turbine. Equations (25) and (26) calculate the stagnation temperature and pressure exiting the high-pressure turbine and entering the low-pressure turbine. Similarly, Eqs. (27) and (28) calculate the stagnation temperature and pressure exiting the low-pressure turbine. Losses which occur due to the mechanical and component efficiency of the turbine are accounted for in these equations as well.

$$T_{05} = T_{04} + \left[\frac{W_C^{HP}}{\eta_m (1 + f_{actual}) \cdot C_{pog}}\right] \tag{25}$$

$$P_{05} = P_{04}\left\{1 - \left[\frac{1-\left(\frac{T_{05}}{T_{04}}\right)}{\eta_t}\right]\right\}^{\frac{\gamma_g}{\gamma_g - 1}} \tag{26}$$

$$T_{06} = T_{05} + \left[\frac{W_C^{LP}}{\eta_m(1+f_{actual})\cdot C_{pog}}\right] \tag{27}$$

$$P_{06} = P_{05}\left\{1 - \left[\frac{1-\left(\frac{T_{06}}{T_{05}}\right)}{\eta_t}\right]\right\}^{\frac{\gamma_g}{\gamma_g - 1}} \tag{28}$$

After the stages of the turbine, the core stream and the auxiliary stream will reunite and mix prior to exhausting through the nozzle. In Eq. (29), the stagnation temperature of the mixed streams in calculated by manipulating conservation of energy, conservation of mass, and the first law of thermodynamics. Similarly, in Eq. (30), the stagnation pressure is a mass-weighted average of the two streams mixing.

$$T_{07} = \frac{B(1+f_{aux})T_{08} + (1+f_{actual})T_{06}}{B(1+f_{aux}) + (1+f_{actual})} \tag{29}$$

$$P_{07} = \frac{B(1+f_{aux})P_{08} + (1+f_{actual})P_{06}}{B(1+f_{aux}) + (1+f_{actual})} \tag{30}$$

Once the two streams have mixed into one, the new stream will exit through a converging nozzle. In Eq. (31), a ratio is set up to test if the nozzle is choked. If P^*/P_{07} is greater than or equal to P_a/P_{07}, then the nozzle is choked meaning the Mach number at the exit is 1. Subsequently, Eqs. (32) to (35) calculate the exit flow static pressure, static temperature, density, and velocity, respectively.

$$\frac{P^*}{P_{07}} = \left\{1 - \frac{1}{\eta_N}\left[1 - \left(\frac{2}{\gamma_g - 1}\right)\right]\right\}^{\frac{\gamma_g}{\gamma_g - 1}} \tag{31}$$

$$P_e = P_{07}\left(\frac{P^*}{P_{07}}\right) \tag{32}$$

$$T_e = T_{07}\left(\frac{2}{\gamma_g + 1}\right) \tag{33}$$

$$\rho_e = \frac{P_e}{R_g \cdot T_e} \tag{34}$$

$$V_e = M_e\sqrt{\gamma_g \cdot R_g \cdot T_e} \tag{35}$$

Conversely, if P^*/P_{07} is less than or equal to P_a/P_{07}, then the nozzle is not choked. This means that the exit pressure is equal to the ambient pressure. The exit flow conditions for the static temperature, density, Mach number, and velocity are calculated in Eqs. (36) to (39).

$$T_e = T_{07}\left\{1 - \eta_N\left[1 - \left(\frac{P_e}{P_{07}}\right)^{\frac{\gamma_g - 1}{\gamma_g}}\right]\right\} \tag{36}$$

$$\rho_e = \frac{P_e}{R_g \cdot T_e} \tag{37}$$

$$M_e = \sqrt{\left[\left(\frac{T_{07}}{T_e}\right) - 1\right]\left(\frac{2}{\gamma_g + 1}\right)} \tag{38}$$

$$V_e = M_e\sqrt{\gamma_g \cdot R_g \cdot T_e} \tag{39}$$

The last step of this parametric study is to calculate the performance and efficiency of this engine. Equations (40) and (41) calculate Fs and TSFC. In Eq. (42), the heating value of the fuel is converted from kJ/kmol to J/kg. Lastly, Eqs. (43) to (45) are used to calculate the propulsive, thermal, and overall efficiency, respectively. Conventionally, propulsive efficiency is defined as the ratio of thrust power to the rate of addition of kinetic energy, and thermal efficiency is defined as the ratio of the rate of addition of kinetic energy to the rate of total energy consumption. These are approximations that neglect to account for the rate of addition of pressure energy [6]. Since the TurboAux is utilizing a purely converging nozzle which has choked flow in every case studied, the pressure energy is not negligible. It was necessary to adjust the conventional equations for propulsive and thermal efficiency to account for the increase in pressure energy. This is outlined in Eqs. (43) and (44).

$$F_s = [(1 + f_o)V_e - V_a] + \left[(P_e - P_a)\left(\frac{1+f_o}{\rho_e \cdot V_e}\right)\right] \tag{40}$$

$$TSFC = \frac{3600 \cdot f_o}{F_s} \tag{41}$$

$$HV = \frac{-Hrp_f \cdot 1000}{M_{fuel}} \tag{42}$$

$$\eta_{prop} = \frac{F_s \cdot V_a}{\left[(1+f_o)\frac{V_e^2}{2} - \frac{V_a^2}{2}\right] + \left[(P_e - P_a)\left(\frac{1+f_o}{\rho_e \cdot V_e}\right)\right]^2} \tag{43}$$

$$\eta_{th} = \frac{\left[(1+f_o)\frac{V_e^2}{2} - \frac{V_a^2}{2}\right] + \left[(P_e - P_a)\left(\frac{1+f_o}{\rho_e \cdot V_e}\right)\right]^2}{f_o \cdot HV} \tag{44}$$

$$\eta_o = \eta_{prop} \cdot \eta_{th} = \frac{F_s \cdot V_a}{f_o \cdot HV} \tag{45}$$

VI. Simulation, Results and Discussion

With the intent to evaluate performance, the thermodynamics of the low-bypass turbofan and the TurboAux engine were modeled and simulated with the use of a computer program. The engines were analyzed under the scenario where the optimal combinations of the FPRs and bypass ratios were adopted for each configuration. The simulations were carried out to understand which conditions provided optimal performances with respect to minimizing the increase in TSFC while aiming to maximize the increase in Fs. The performance of the engines is summarized in Figs. 3 and 4 and the values are tabulated in Tables 2 and 3. Table 4 tabulates the respective increases and decreases in the different performance parameters of both the low-bypass turbofan and the TurboAux. Figure 5 illustrates the changes in Fs and TSFC of both the TurboAux and a similarly configured low-bypass turbofan with respect to bypass ratio.

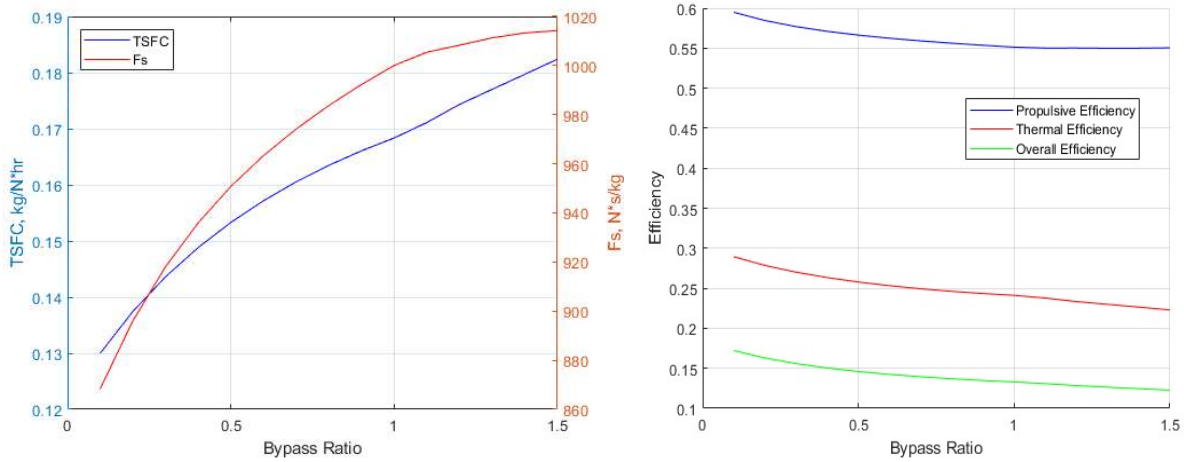

(a) **(b)**

Fig. 3 Performance Analysis – (a) TurboAux: TSFC Vs Fs as a Function of Bypass Ratio, (b) TurboAux: Efficiency Vs Bypass Ratio

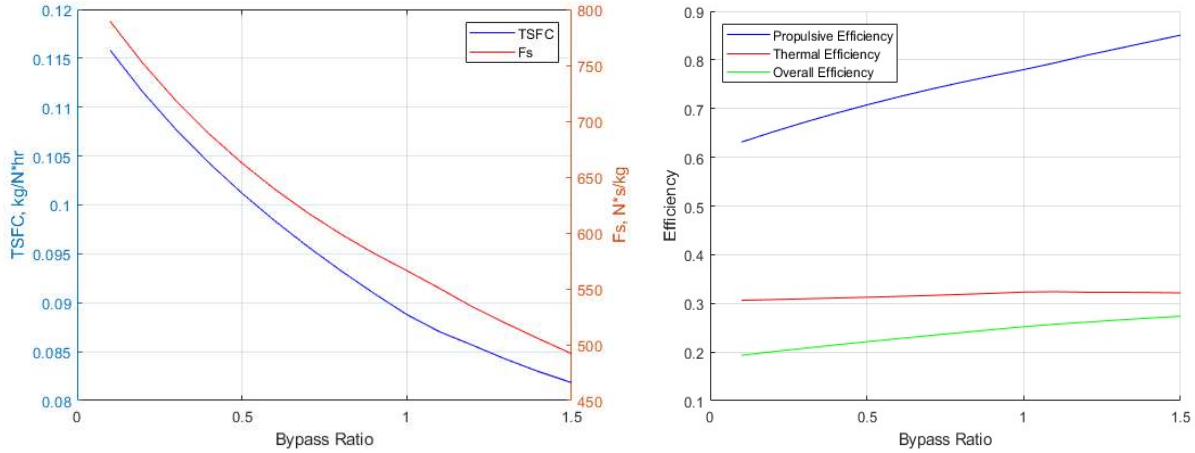

(a) **(b)**

Fig. 4 Performance Analysis – (a) Turbofan: TSFC Vs Fs as a Function of Bypass Ratio, (b) Turbofan: Efficiency Vs Bypass Ratio

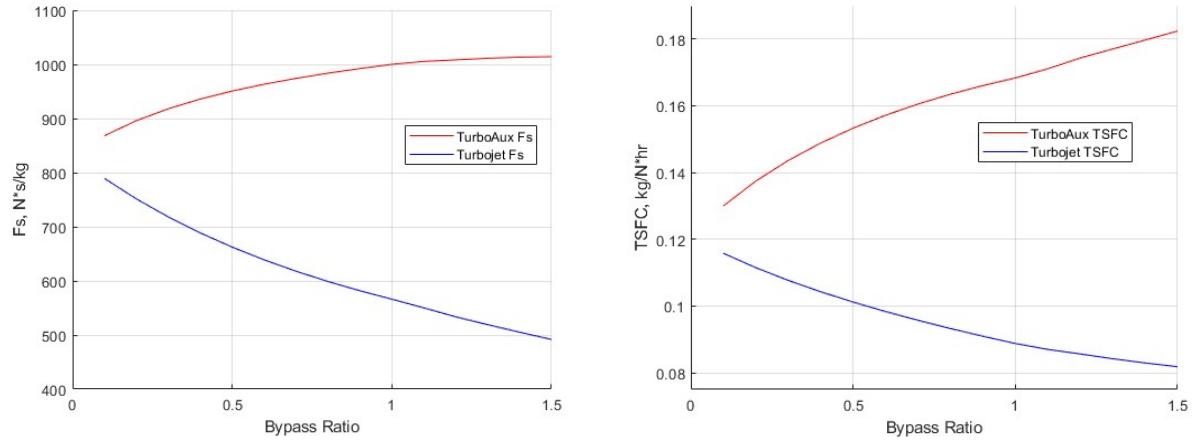

(a) **(b)**

Fig. 5 Performance Analysis – (a) TurboAux Fs vs Turbofan Fs as a Function of Bypass Ratio, (b) TurboAux TSFC vs Turbofan TSFC Fs as a Function of Bypass Ratio

Table 2. Optimized Turbofan Engine Configuration and Corresponding Results

Bypass Ratio	ABPR	TSFC (kg/N*hr)	Fs (N*s/kg)	Propulsive Efficiency	Thermal Efficiency	Overall Efficiency
0.1	7	0.115819	789.260	63.12 %	30.61 %	19.32 %
0.2	7	0.111510	751.444	65.21 %	30.78 %	20.07 %
0.3	7	0.107705	718.150	67.17 %	30.94 %	20.78 %
0.4	7	0.104294	688.660	69.02 %	31.09 %	21.46 %
0.5	7	0.101199	662.408	70.76 %	31.26 %	22.12 %

0.6	7	0.098359	638.937	72.39 %	31.43 %	22.75 %
0.7	7	0.095729	617.874	73.93 %	31.62 %	23.38 %
0.8	7	0.093274	598.906	75.37 %	31.84 %	24.00 %
0.9	7	0.090968	581.768	76.73 %	32.07 %	24.60 %
1	7	0.088790	566.235	78.00 %	32.32 %	25.21 %
1.1	6.7	0.087024	550.230	79.40 %	32.39 %	25.72 %
1.2	6.2	0.085650	533.707	80.93 %	32.29 %	26.13 %
1.3	5.9	0.084229	519.180	82.32 %	32.28 %	26.57 %
1.4	5.6	0.082958	505.260	83.70 %	32.23 %	26.98 %
1.5	5.3	0.081832	491.835	85.08 %	32.15 %	27.35 %

Table 3. Optimized TurboAux Engine Configuration and Corresponding Results

Bypass Ratio	ABPR	TSFC (kg/N*hr)	Fs (N*s/kg)	Propulsive Efficiency	Thermal Efficiency	Overall Efficiency
0.1	7	0.129998	868.331	59.48 %	28.94 %	17.22 %
0.2	7	0.137441	896.059	58.46 %	27.86 %	16.28 %
0.3	7	0.1436147	918.070	57.69 %	27.01 %	15.58 %
0.4	7	0.1488337	935.942	57.10 %	26.33 %	15.04 %
0.5	7	0.1533048	950.770	56.63 %	25.78 %	14.60 %
0.6	7	0.1571718	963.330	56.24 %	25.32 %	14.24 %
0.7	7	0.1605389	974.182	55.91 %	24.94 %	13.94 %
0.8	7	0.1634849	983.736	55.62 %	24.61 %	13.69 %
0.9	7	0.1660716	992.291	55.36 %	24.34 %	13.48 %
1	7	0.1683487	1000.068	55.13 %	24.12 %	13.29 %
1.1	6.7	0.1710977	1005.445	55.01 %	23.78 %	13.08 %
1.2	6.2	0.1743308	1008.312	55.02 %	23.34 %	12.84 %
1.3	5.9	0.1770197	1011.313	54.99 %	22.99 %	12.64 %
1.4	5.6	0.1797008	1013.292	55.00 %	22.65 %	12.45 %
1.5	5.3	0.182405	1014.266	55.04 %	22.29 %	12.27 %

Table 4. Performance Percentages

	TSFC	Fs	Propulsive Efficiency	Thermal Efficiency	Overall Efficiency
Turbofan	-29 %	-38 %	+35 %	+5 %	+42 %
TurboAux	+40 %	+17 %	-7 %	-23 %	-29 %

The results presented in the previous section model the performance of the novel TurboAux engine in comparison to a conventional turbofan engine. In the conventional low-bypass turbofan engine, a few trends became apparent. As bypass ratio increased, TSFC decreased at a significant cost to Fs, but propulsive, thermal, and overall efficiency increased as expected. This is illustrated in Fig. 4. Conversely, in the TurboAux, as bypass ratio increased, TSFC increased as did Fs, but all three efficiencies decreased. These trends are illustrated in Fig. 3. It is apparent that the augmentation of an auxiliary combustion chamber in the bypass stream of a low-bypass turbofan engine will significantly increase the thrust capabilities of the engine at the cost of increased fuel consumption and lower efficiency. As bypass ratio increased, the turbofan model resulted in a 29% decrease in TSFC and a 38% decrease in Fs, but the overall efficiency increased by 42%. The TurboAux model showed a 40% increase in TSFC and a 17% increase in Fs, but the overall efficiency suffered a 29% decrease. Figure 5 further illustrates the performance of these engines compared to one another.

VII. Conclusion and Future Work

The increase of bypass ratio in a low-bypass turbofan engine lowers TSFC and increases overall efficiency but at the cost of a significant loss in Fs. The premise of this research and the conception of this novel engine design (TurboAux engine) aims to investigate the possibility of considerably increasing the thrust capability of an engine while keeping the fuel consumption steady and manageable. The results presented show that while Fs is increased, so is TSFC. Applications for this engine should be considered in scenarios where lowering fuel consumption is not the primary objective as is the case with commercial flights. This subsonic novel engine makes the case for its application in charter aircraft and close-air-support aircraft as well as a myriad of other applications.

As part of the future work, the authors are working on studying the implementation of a TurboAux engine in aircrafts with engines whose capacities are comparable. The authors are also studying the TurboAux engine as an alternative to a turbojet or turbofan engine with an afterburner. These results will be presented as a journal publication of the TurboAux engine.

References

[1] Raymer, D.P., *Aircraft Design: A Conceptual Approach*, 5th ed., AIAA Education Series; American Institute of Aeronautics & Astronautics: Reston, VA, USA, 2012.

[2] MacIsaac, B., and Langston, R., *Gas Turbine Propulsion Systems*, 1st ed., Wiley: Hoboken, NJ, USA, 2011.

[3] Cohen, H., Rogers, G.F.C., and Saravanamuttoo, H.I.H., *Gas Turbine Theory*, 3rd ed., John Wiley & Sons, New York, 1987, Chap. 3.

[4] Asundi, S.A., and Ali, S.F., "Parametric Study of a Turbofan Engine with an Auxiliary High-Pressure Bypass," *International Journal of Turbomachinery, Propulsion and Power*, Vol 4, No. 1, Jan 2019

[5] Campbell, A.S., *Thermodynamic Analysis of Combustion Engines*, 1st ed., Wiley: Hoboken, NJ, USA, 1979.

[6] Hill, P., and Peterson, C., *Mechanics and Thermodynamics of Propulsion*, 2nd ed., Prentice Hall, USA, 1992.